Bayesian hierarchical modelling of nitrate concentration in a forest stream affected by large-scale forest dieback

Hoseung Jung[1], Cornelius Senf[1,2], Burkhard Beudert[3], and Tobias Krueger[1]

[1]IRI THESys, Humboldt-Universität zu Berlin.

[2]Ecosystem dynamics and forest management group, School of Life Sciences, Technical University of Munich

[3]Bavarian Forest National Park.

Corresponding author: Hoseung Jung (hoseung.jung@hu-berlin.de)

Key Points:

- Pulse of nitrate export from a forest catchment in response to bark beetle infestation followed by recovery of nutrient retention capacity
- Bayesian hierarchical model predicting stream nitrate concentration dynamics with discharge and water temperature
- Mechanistic explanation of concentration-discharge-temperature relationship to assist interpretation of the regression analysis

Abstract

The ecosystem function of vegetation to attenuate riverine export of nutrients is of substantial importance for securing water quality. This ecosystem function is at risk of deterioration due to an increasing risk of large-scale forest dieback under climate change. The present study explores the response of the nitrogen (N) cycle of a forest catchment in the Bavarian Forest National Park, Germany, in the face of a severe bark beetle (*Ips typographus*) outbreak and resulting large-scale forest dieback. Outbreaks of bark beetle killed the dominant tree species Norway spruce (*Picea abies*) in up to 55 % of the area. A Bayesian hierarchical model that predicts stream NO_3 concentration (C) with discharge (Q) and water temperature (T) as predictors (C-Q-T relationship) was found as the best fitting model. This informed top-down development of a catchment model to explain the C-Q-T relationship so that the annually-varying model parameter estimates provide mechanistic interpretations of the catchment processes. NO_3 concentration increased after the dieback because N was released from the decaying fine litter of trees beyond the capacity of the terrestrial vegetation and riparian zone to regulate the nutrient export. Within a decade after the dieback, the released N was flushed out and nutrient retention capacity was restored with the regrowth of the vegetation. Greater understanding of canopy mortality due to climate change and other anthropogenic impacts are required to mitigate the deterioration of nutrient retention and prevent nutrient loss.

1 Introduction

Water is important in the global nutrient cycle, both as a transport agent and as a medium for biogeochemical reactions in soil, ground and surface waters. Large aquatic ecosystems rely on the nutrient supply via hydrological pathways. However, when nutrients are present in water at excessive concentrations, they can cause environmental harm such as eutrophication and hypoxia, leading to deterioration of water quality for ecosystems and human use [*Hilton et al.*, 2006; *Xu et al.*, 2014]. Vegetation is a crucial mediating agent in the cycling of water as it intercepts precipitation, and transpires and regulates evaporation and groundwater flow [*Harman et al.*, 2011; *Adams et al.*, 2012]. Nutrient exports are also regulated by vegetation growth which assists in biogeochemical processes that retain nutrients in soils or release them [*Botter et al.*, 2010; *Gall et al.*, 2013].

Forest catchments, whose hillslopes and riparian areas are covered largely by vegetation, are especially effective at regulating nutrient exports. Since forests account for approximately 30 % of global land cover [*Hansen et al.*, 2013], the nutrient regulation of forest catchments provides a crucial ecosystem function for the conservation of water resources and ecosystems worldwide. In recent decades, concerns have grown about large-scale pulses of forest dieback due to drought and insect infestation [*Allen et al.*, 2010; *Seidl et al.*, 2017]. Although tree mortality and pulses of increased mortality are natural processes, large-scale forest diebacks can undermine the nutrient regulating function of forests and thus threaten ecosystem and drinking water quality.

In a catchment experiencing pulses of increased forest mortality, export of nitrogen (N) is of key concern since inorganic N is leached easily [*Gundersen et al.*, 2006] and hence in-stream concentrations respond drastically to diebacks [*Hartmann et al.*, 2016]. *Vitousek and Reiners* [1975] were among the first to explain that an ecosystem loses nutrients after a forest dieback,

but then retains them more effectively than before the dieback as biomass accumulates again during the following succession. Several studies have since observed increases of inorganic N exports in forest catchments affected by forest diebacks caused by bark beetle infestation [*Biederman et al.*, 2016], wildfire [*Betts and Jones Jr.*, 2009], windthrow [*Hartmann et al.*, 2016] and also in watersheds affected by clear-cut harvest [*Pardo et al.*, 1995].

Outbreaks of the European spruce bark beetle (*Ips typographus* Linnaeus) have increased in frequency and magnitude in Central Europe over recent decades due to the combined effects of past land use legacies and climate change [*Seidl et al.*, 2011; *Senf et al.*, 2017], leading to an observable increase in canopy mortality [*Senf et al.*, 2018]. For instance, the Bavarian Forest National Park, Germany, experienced two large-scale bark beetle outbreaks between 1990 and 2010 [*Kautz et al.*, 2011], which led to the dieback of most of the bark beetle's host tree Norway spruce (*Picea abies* (L.) H.Karst.). The dieback of Spruce caused an increase in the export of nitrate (NO_3), while at the same time benefitting biodiversity since the mortality of this dominant tree species created canopy gaps and provided new niches (i.e., deadwood) for many forest dwelling species [*Gundersen et al.*, 2006; *Beudert et al.*, 2014]. While the forest dieback has been unprecedented, recent studies have shown the high resilience of the system, with the forest returning after several years post dieback [*Zeppenfeld et al.*, 2015; *Senf et al.*, 2019]. Further, unlike most forests of Europe that are intensively managed, the bark beetle outbreak within the core zone of the National Park was protected without any management measure, leading to a unique opportunity for research on the effects of forest diebacks on ecosystem processes, such as the responses of the N cycle of a whole forest catchment to natural bark beetle induced forest diebacks.

Nutrient export from a catchment is complicated by heterogeneous sources, dynamic pathways and variable biogeochemical processes [*Basu et al.*, 2011; *Musolff et al.*, 2015]. It is challenging to monitor the relevant processes in hillslopes and streams across an entire catchment. In practice, nutrient concentration is most often monitored in streams representing integrated effects of catchment processes and enabling quantification of downstream export. The relationship of solute concentration with discharge (C-Q relationship) and its variation in space and time has proven a particularly useful indicator of catchment processes [*Musolff et al.*, 2015; *Rose et al.*, 2018; *Zhi et al.*, 2019]. Previous studies showed that the C-Q relationship relies on the reactivity of the solute and spatial correspondence between the source areas and discharge [*Seibert et al.*, 2009; *Basu et al.*, 2011; *Thompson et al.*, 2011]. These studies have followed a data-driven, or 'top-down' modelling approach [*Sivapalan et al.*, 2003] that aims at accounting for the dominant catchment processes using parsimonious model structures that are commensurate with the often limited availability of data [*Krueger et al.*, 2007].

Regression models have proven particularly efficient in screening and investigating the relationships of nutrient concentrations with other environmental variables [*Chavez and Service*, 1996; *Clark et al.*, 2004b; a; *Exner-Kittridge et al.*, 2016]. Where these data and relationships relate to disparate scales then an hierarchical model is called for, with the Bayesian hierarchical framework being the most flexible and coherent. Bayesian hierarchical modeling has been applied to hydrochemical data to predict the behavior of aquatic environments such as nutrient concentrations [*Xia et al.*, 2016], algal blooms [*Obenour et al.*, 2014; *Cha et al.*, 2016; *Cha et al.*, 2017], dissolved oxygen [*Borsuk et al.*, 2001; *Stow and Scavia*, 2008] and salinity [*Webb et al.*, 2010]. *Borsuk et al.* [2001] and *Stow and Scavia* [2008] applied mechanistic models in a Bayesian hierarchical framework combining the strengths of mechanistic and statistical modeling;

making predictions based on process knowledge while estimating parameters empirically from data.

The aim of this study was to investigate the response of the N cycle of a catchment within the Bavarian Forest National Park, the Grosse Ohe catchment, to the bark beetle induced forest dieback using in-stream monitoring data and Bayesian hierarchical modeling in top-down fashion. We hypothesized: (1) that NO_3 concentrations in forest streams would increase due to the loss of nutrient retention capacity in forests affected by large-scale mortality; (2) that the nutrient retention would recover after dieback due to the regrowth of vegetation, indicating an overall resilient ecosystem. To test those hypotheses, we first developed a Bayesian hierarchical model through model comparison to investigate temporally variant relationships between stream NO_3 concentration and other environmental variables. Second, the resultant model structure inspired a parsimonious catchment model that provides mechanistic interpretations of catchment dynamics across sites and years for specifically addressing the hypotheses. The derivation of the parsimonious catchment model, resulting from the initial Bayesian hierarchical model, will be described in the results section. We conclude our analysis by correlating model parameters with an independent remote sensing based proxy of vegetation activity, the normalized difference vegetation index (NDVI) in order to guide parameter interpretation and independently evaluate the plausibility of the mechanistic model.

2 Materials and Methods

2.1 Study Area and Measurements

Grosse Ohe is a headwater catchment located in the Bavarian Forest National Park, Germany, with a size of 19.1 km^2 and a mountainous topography with 11.1° mean slope at altitudes of 770 – 1447 m above sea level. 98 % of the catchment area is forested, and human management was excluded since at least the 1970s (i.e., since establishment of the National Park). Norway spruce dominated forests cover approximately 70 % of area, with the remaining area being dominated by European beech (*Fagus sylvatica* L.). Stream hydrochemistry was monitored at the outlets of Grosse Ohe (48°56'17.99" N, 13°24'45.13" E) and its two nested subcatchments Markungsgraben (48°57'20.89" N, 13°25'35.8" E, 1.1 km^2) and Forellenbach (48°56'33.61" N, 13°25'10.63" E, 0.7 km^2). The forest dieback was most severe in Markungsgraben (mortality on approximately 82 % of the catchment area) compared to Forellenbach (mortality on approximately 57 % of the area) and the entire catchment Grosse Ohe (mortality on approximately 55 % of the area). A map displaying the study catchment with the forest dieback, the streams and the monitoring stations can be found in Figure S1 of the Supporting Information.

The hydrochemical measurements include water level and concentrations of nitrogen (N), phosphorus, organic carbon and dissolved oxygen (DO), pH, conductivity and water temperature. Water levels were measured quasi-continuously (every 15 minutes) and converted to discharges via rating curves. Baseflow was separated from the discharge with a digital filter algorithm available in the R package ‘EcoHydRology’ [*Fuka et al.*, 2018]. The baseflow index was computed as the proportion of baseflow relative to discharge. Temperature, pH, DO and electric conductivity were measured every minute. All sub-daily data were aggregated to daily means to

match the instantaneous sampling. Instantaneous samples for chemical analyses were taken manually every two weeks at Grosse Ohe and Markungsgraben and weekly at Forellenbach. The samples were analyzed monthly in the laboratory to determine nutrient concentrations according to DIN/EN/ISO. The monitoring programs started in 1977 for Grosse Ohe, 1988 for Markungsgraben and 1990 for Forellenbach. Water temperature was only available from 2002 and DO was not available at Forellenbach. Further details of the geographical and hydrometeorological characteristics and monitoring of the area are described in *Beudert and Gietl* [2015].

The annual percent of forest canopy experiencing dieback was manually identified via airborne image analysis (see *Heurich et al.* [2010] for details). We further acquired annual NDVI time series from the United States Geological Survey Landsat satellite archive for the years 1986 to 2016 (see *Senf et al.* [2017] for details on image processing). We used the NDVI time series as independent proxy of vegetation activity, i.e., indicating the loss and subsequent recovery of photosynthetic activity during and after the bark beetle outbreak. We averaged annual NDVI observations at the catchment level and applied a smoothing model (generalized additive model) to account for variable phenology between Landsat acquisitions that potentially overshadow the more subtle longer-term trends associated with forest dieback and recovery [*Senf et al.*, 2019].

2.2 Bayesian Hierarchical Regression Model

The concentrations of NO_3 in the streams of Grosse Ohe and its nested subcatchments were predicted by regression models in a Bayesian hierarchical framework. Candidate regression models with different sets of predictors were compared (see below). The slopes and intercepts of the regression models were allowed to vary each hydrological year (starting in November):

$$\log(C_i) = \beta_{0,j} + \beta_{1,j}X_{1,i} + \beta_{2,j}X_{2,i} + \cdots + \beta_{P,j}X_{P,i} + \varepsilon_i \quad (1)$$

where C_i and $X_{\{1, 2, \ldots, P\},i}$ are *i*th measurements of stream NO_3 concentration and the corresponding values of the *P* predictors, respectively. $\beta_{0,j}$ and $\beta_{\{1, 2, \ldots, P\},j}$ are the intercept and slope parameters for the *P* predictors, respectively, for the *j*th year. ε_i is the residual error. By modelling ε_i as a normal distribution and taking the logarithm of the response C_i, NO_3 concentration was effectively modelled as a lognormal distribution. The model parameters $\beta_{0,j}$ $\beta_{\{1, 2, \ldots, P\},j}$ and ε_i were partially pooled across the hydrological years to control over-fitting. That is, these parameters were modelled as realizations of common distributions, whose parameters were simultaneously inferred from the data:

$$\beta_{m,j} \sim \text{Normal}(\mu_{\beta_m}, \sigma^2_{\beta_m}), \text{ for } m = 0, 1, 2, \ldots, P \quad (2)$$

$$\varepsilon_i \sim \text{Normal}(0, \sigma^2_{\varepsilon_j}) \quad (3)$$

$$\sigma_{\varepsilon_j} \sim \text{Normal}(\mu_{\sigma_\varepsilon}, \sigma^2_{\sigma_\varepsilon}) \quad (4)$$

where $\mu_{\beta m}$ is the mean of the regression parameter β_m and $\sigma^2_{\beta_m}$ is the variance of the "random effect" that models the variability of β_m between years.

The residual error for the jth year ε_j is considered normally distributed with mean zero and variance $\sigma^2_{\varepsilon_j}$, which varies between years according to a normal distribution with mean μ_{σ_ε} and variance $\sigma^2_{\sigma_\varepsilon}$. Weakly informative Normal(0,5) prior distributions were assigned to μ_{β_m} with

m = 0, 1, 2, …, P. Weakly informative Inverse-gamma(0.01, 0.01) priors were assigned to σ_{β_m}, μ_{σ_ε} and $\sigma_{\beta_\varepsilon}$ as these parameters are bound to be positive [*Gelman*, 2006]. Allowing the parameters and residual error term to vary temporally in the Bayesian hierarchical framework reflects the possibility that the processes that regulate stream NO_3 vary over time, but shrunk towards a common mean so as to avoid over-fitting. From this temporal variation of model parameters we hope to extract information on catchment dynamics in top-down fashion (see 2.3).

The partially-pooled models were compared with pooled and non-pooled models. In the pooled version, the parameters were constant over the years. In the non-pooled version, the parameters were estimated individually for each year, without common prior distributions. The joint posterior distribution of the parameters was simulated using Markov Chain Monte Carlo (MCMC) methods available in Stan [*Carpenter et al.*, 2017] and implemented in the R environment [*R Core Team*, 2018; *Stan Development Team*, 2018]. 1000 realizations of the model parameters and predicted NO_3 were generated from their posterior distributions after 1000 burn-in samples in four parallel chains. Code files of the partially pooled, non-pooled and pooled models are provided in the Supporting Information.

The candidate regression models with different sets of predictors were compared for their predictive accuracy by means of k-fold cross validation. The data sets of each site were randomly divided into 10 subsets y_k, for k = 1, 2, …, 10, with even numbers of data point. The models were fit to a training data set $y_{(-k)}$ and subsequently used for predicting the NO_3 concentrations of the validation set y_k. This process was repeated for each subset and the posterior distributions of the predictions were used to calculate the expected log pointwise predictive density (ELPD), a relative measure of predictive performance under out-of-sample conditions [*Vehtari et al.*, 2017].

2.3 Top-down Catchment Model

In a second step, the regression analysis (2.2) was interpreted with a parsimonious process-based model of NO_3 export at the catchment scale in top-down fashion [*Sivapalan et al.*, 2003]. Equations describing the processes of nutrient export were defined using the predictor variables of the best fit regression model and based on the literature. In this way, mechanistic implications of the regression model could be derived. As a first step towards explaining the temporal variation of the parameters in relation to the bark beetle induced forest dieback, correlations between annual parameter estimates and the NDVI as independent proxy of vegetation activity were quantified using Spearman's rank correlation coefficient (ρ).

3 Results

3.1 Temporal Variations of Vegetation Canopies and Hydrochemical Responses

Over the entire catchment, Grosse Ohe, the bark beetle infestation occurred in two waves between 1994 and 2009, killing Norway spruce trees with annual mortality rates peaking in 1999 (12 % of area) and 2006 (5 % of the area). The infestation occurred in Forellenbach in 1994 – 2000 and 2002 – 2008 with maximum annual mortalities of 12 % (1999) and 7 % (2006), respectively. The bark beetle outbreak led to highest mortality rates in the Markungsgraben catchment between 1995 and 2001, where a maximum annual mortality rate of 39 % was

recorded in 1997 (Figure 1a). The annual NDVI time series well fitted the recorded mortality, with largest negative deviations in annual NDVI (i.e., annual vegetation activity) for Markusgraben (Figure 1a), but with rapid recovery of vegetation activity after the main mortality waves for all catchments. The rapid return of vegetation including spruce trees is also well documented in other studies, suggesting that the forests recovered from the bark beetle induced spruce dieback [*Svoboda et al.*, 2010; *Zeppenfeld et al.*, 2015; *Senf et al.*, 2019].

Discharge was highly variable over the course of the bark beetle outbreaks (Figure 1b), with a discharge yield of 0.40 – 58.5 mm day^{-1} across all sites and over the entire monitoring period. In volumetric terms, the largest flux occurred at the most downstream monitoring station of Grosse Ohe (0.59 ± 0.66 m^3 s^{-1} (mean ± standard deviation)), followed by the upstream stations Markungsgraben (0.05 ± 0.06 m^3 s^{-1}) and Forellenbach (0.02 ± 0.02 m^3 s^{-1}). The baseflow indices were 49 %, 64 % and 54 % in Markungsgraben, Forellenbach and Grosse Ohe, respectively. The baseflow contribution decreased with mean slope (16.1° in Markungsgraben, 8.4° in Forellenbach and 11.1° in Grosse Ohe).

Annual mean stream NO_3 concentration increased until 2000 at Markungsgraben, 2003 at Forellenbach and 2002 at Grosse Ohe, during the first halves of the dieback periods (Figure 1c). Correlation coefficients ρ between annual mean NO_3 and NDVI were -0.82 – -0.88 across the sites, meaning that stream NO_3 decreased when the vegetation was active (compare Figure 1a and c). NO_3 showed minima in the growing season (May – September) and maxima in the dormant season. However, under elevated NO_3 concentrations during the dieback, the seasonal pattern vanished in 2004 at Forellenbach and 1998 and 2003 at Markungsgraben. We define the years with decreased NDVI and elevated NO_3 (1995 – 2003 at Markungsgraben, 1997 – 2009 at Forellenbach and Grosse Ohe) as dieback phase and the preceding and following years as pre- and post-dieback phases, respectively.

The water temperature ranged between -0.01 and 20.1 °C, while 95 % of the values were within 0.03 – 13.0 °C, with means increasing above 5 °C in May – October (Figure 1d). Temperature measurements at the three sites were highly correlated ($p < 0.01$, r^2 0.83 – 0.96), meaning that the water temperature reflects the regional climate of the area. Annual mean temperatures showed clear and steady increasing trends across the sites (Mann-Kendall test $p < 0.05$).

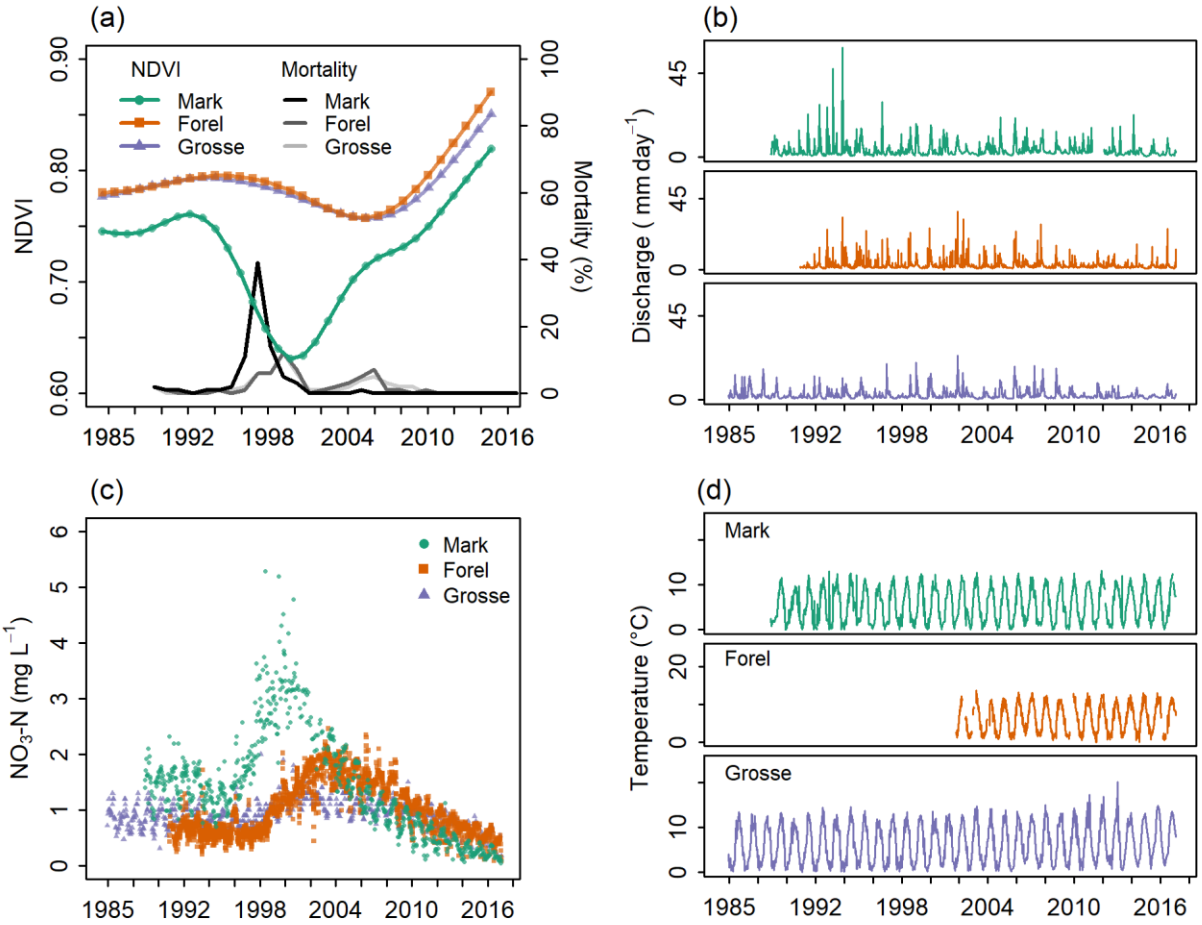

Figure 1. (a) Normalized difference vegetation index (NDVI), mortality, (b) discharge, (c) nitrate concentration (NO_3) and (d) water temperature of Markungsgraben, Forellenbach and Grosse Ohe.

3.2 Selection of Regression Model

The regression models with different sets of predictors and pooling setups were compared using ELPD, with greater values signifying better predictive performance. Both original and log-transformed data were tested, and the ELPDs of the best fitting models are presented in Table S1. C-Q-T (concentration-discharge-temperature) model with partially pooled parameters showed the greatest ELPD values across the sites, outperforming even models with three predictors. The C-Q-DO model (concentration-discharge-dissolved oxygen) was more accurate than the C-Q-T model at Grosse Ohe but the enhancement in ELPD was low (0.01). DO was correlated with water temperature with ρ = -0.72 at Markungsgraben and ρ = -0.97 at Grosse Ohe because of the increased solubility of oxygen in water at low temperatures [*Wetzel*, 2001]. No DO data were available for Forellenbach.

As a result, the C-Q-T model was selected for further analysis. The equation can be written as

$$\log(C_i) = \beta_{0,j} + \beta_{1,j} \cdot logQ_i + \beta_{2,j} \cdot T_i + \varepsilon_i \quad (5)$$

3.3 Development of Top-down Catchment Model

A mechanistic model explaining the variation of in-stream NO_3 with discharge and water temperature was developed based on the relationships between the variables suggested by the selected regression model. This mechanistic model is a lumped model that conceptualizes the processes within the catchment as a single unit. Hence the parameters of this model represent the characteristics of the entire catchment without spatial heterogeneity; they are so called "effective" parameters.

The relationship of log(NO_3) and water temperature in the regression model suggests that NO_3 is processed in first-order reactions with rates affected by water temperature. In the riparian zone, the NO_3 is either removed by assimilation of plants and microorganisms or by denitrification, or produced from organic N via mineralization and nitrification [*Stoddard*, 1994; *Zheng et al.*, 2016]. Among different possibilities of defining the riparian zone, we define it as the soil adjacent to the stream and in the hyporheic zone, where nutrients are retained actively via biogeochemical processes [*Lowrence et al.*, 1983; *Parkyn*, 2004]. The vertical concentration profile of NO_3 in the riparian zone is shaped by heterogeneous inputs from the hillslope soils and biogeochemical reactions. It can be expressed as a function of depth z and temperature T as

$$c(z,T) = c_{s0} \cdot e^{kt_rT+fz} \quad (6)$$

where c_{s0} is the initial concentration of NO_3 at the surface layer [mg N L^{-1}], k [$C^{\circ-1}$ s^{-1}] is a rate constant, t_r [s] is the NO_3 residence time and f [m^{-1}] is a shape parameter of the vertical distribution. The biogeochemical processes were assumed to alter the NO_3 concentration in the riparian zone instantaneously or at least within the residence time t_r before the nutrient enters the stream [*Seibert et al.*, 2009] based on literature reviews of rates of N uptake and denitrification [*Stoddard*, 1994; *Masclaux-Daubresse et al.*, 2010].

NO_3 is assumed to be transported laterally from upslope sources through the riparian zone to reach the stream. Lateral water flux at depth z (q) [m^2 s^{-1}] was modeled to decline exponentially [*Seibert et al.*, 2009]:

$$q = q_0 \cdot e^{\lambda z} \quad (7)$$

where λ [m^{-1}] is a shape parameter of the water flux profile and q_0 [m^2 s^{-1}] is the transmissivity at the top of the riparian zone. The hydraulic conductivity of the soil was assumed to be little affected by the forest dieback and thus did not change over the years.

Integration of equation 7 results in an equation for discharge [m^3 s^{-1}] governed by groundwater depth, or depth of the saturated zone below the soil surface:

$$Q = q_0/\lambda \cdot e^{\lambda z} \quad (8)$$

q_0/λ [m^3 s^{-1}] represents the maximum discharge when the soil is saturated (groundwater depth z = 0 m), neglecting overland and preferential flows.

Modifying the model by *Seibert et al.* [2009], averaging the NO_3 flux (concentration times lateral water flux) over depth results in a governing equation of in-stream NO_3

concentration as a function of upslope inputs (represented by c_{s0}), discharge (Q) and water temperature (T):

$$C = \frac{L}{Q} = \frac{\int_{-\infty}^{z_t} qcdz}{\int_{-\infty}^{z_t} qdz} \quad (9)$$

$$\log C = \log[c_{s0}(1+b)^{-1}\left(\frac{\lambda}{q_0}\right)^{b}] + b \cdot \log Q + kt_r T$$

$$= \log S + b \cdot \log Q + kt_r T \quad (10)$$

where z_t is ground water depth at time t, b is f/λ [-] and S is $c_{s0}(1+b)^{-1}(\lambda/q_0)^{b}$. This equation combines the C-Q and C-T relationships into the C-Q-T relationship revealed by the best fit regression model. The rationale of the current model explains the mechanism of the empirical C-Q-T relationship. More details on the derivation and assumptions of equation 6 and 10 can be found in the Supporting Information (Text S1 and S2, respectively).

From the definition of S it follows that

$$c_{s0} = S(1+b)(q_0/\lambda)^{b} \quad (11)$$

This equation can be used for estimating c_{s0}, which is affected by the dynamics of the vegetation and hence potentially sensitive to the bark beetle outbreak.

It is important to note that equations 5 and 10 are analogous to each other. The intercept of the regression model is logS, a compound of four mechanistic parameters; c_{s0}, b, λ and q_0. The slopes of equation 5, β_1 and β_2, correspond to b (= f/λ) and the product of k and t_r of equation 10 (kt_r), respectively. In our hierarchical setup, the soil input c_{s0} can be inferred from the annual estimates of S and b given values of q_0 and λ. The C-Q slope b signifies the vertical profile of NO_3 transport through the riparian zone shaped by hydraulic conductivity (λ) and availability of the nutrient (f). A positive k indicates that the riparian zone is a source of NO_3 and a negative k indicates a sink, while t_r is always equal to or larger than zero. Accordingly, the parameter kt_r represents the rate of removal ($kt_r < 0$ $C^{\circ -1}$) or production ($kt_r > 0$ $C^{\circ -1}$) of NO_3 in the riparian zone. The magnitude of net removal/production is determined both by the biogeochemical reaction (k) and the residence time (t_r). With $kt_r < 0$ $C^{\circ -1}$, NO_3 is lower in summer creating a seasonal pattern because high temperature enhances net NO_3 removal [*Christensen et al.*, 1990; *Clark et al.*, 2004a; *Huber*, 2005]. The seasonal pattern is reversed if $kt_r > 0$ $C^{\circ -1}$ with net NO_3 production magnified by a temperature increase.

3.4 Prediction of Nitrate

The stream NO_3 concentrations predicted by the C-Q-T model corresponded well to the observed concentrations (Figure 2). The root mean square errors (RMSE) were 0.36 [0.33 – 0.40] (mean [95 % credible interval]) mg N L^{-1}, 0.20 [0.19 – 0.22] mg N L^{-1} and 0.18 [0.17 – 0.19] mg N L^{-1} across the years at Markungsgraben, Forellenbach and Grosse Ohe, respectively. The model predicted the seasonal pattern of NO_3 correctly, as well as the disappearance of the seasonal pattern in the dieback phase at Markungsgraben (1997-2001) and Forellenbach (2002). In these years, the two predictors were insufficient to explain the NO_3 dynamics, showing higher RMSEs (0.68 [0.58, 0.80] mg N L^{-1} at Markungsgraben and 1.10 [0.98, 1.19] mg N L^{-1} at Forellenbach). NO_3 at Forellenbach was greatly controlled by discharge, where the concentration

was diluted during storm events. Prediction of NO_3 and further data analysis could not be performed before 2002 at Forellenbach due to the limited availability of temperature data.

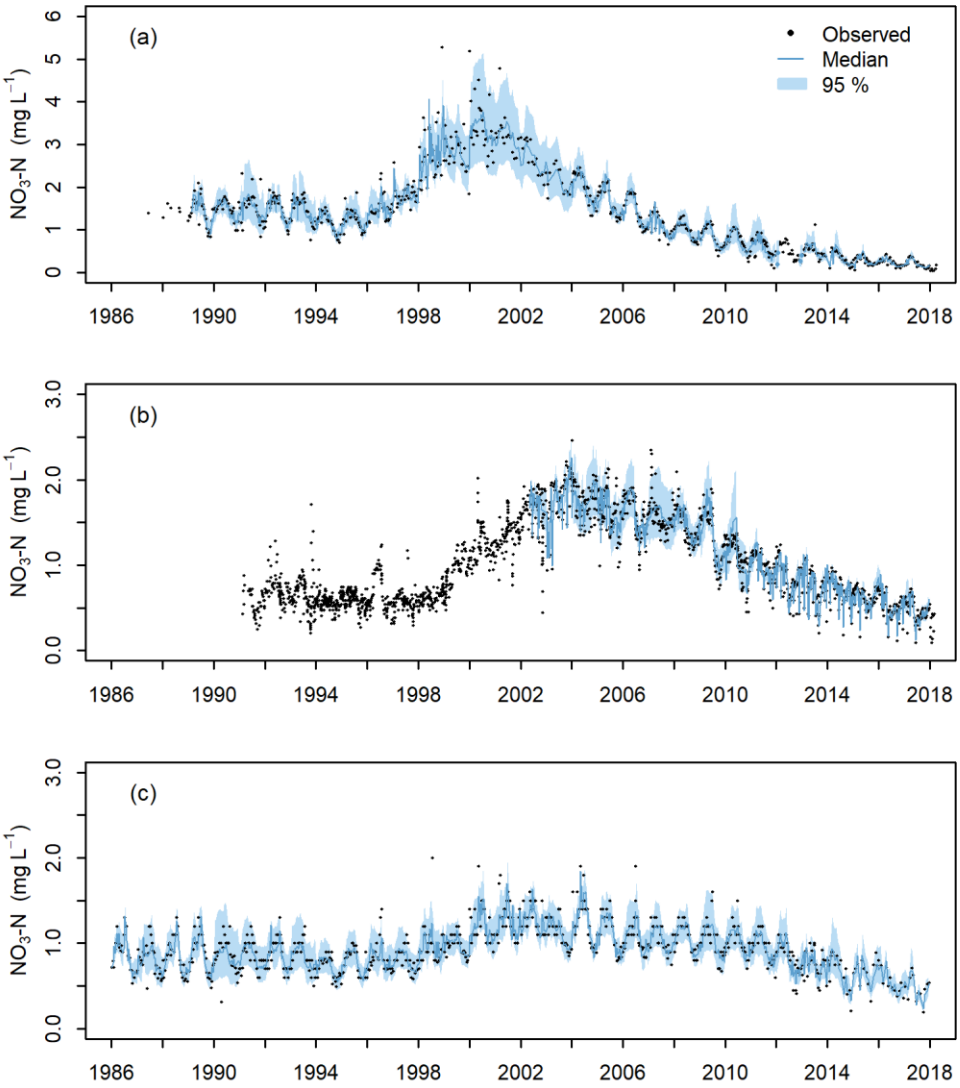

Figure 2. Predicted and observed in-stream nitrate concentrations at the outlets of (a) Markungsgraben, (b) Forellenbach and (c) Grosse Ohe.

Plotting predicted and observed in-stream NO_3 against each other verified the high predictive accuracy of our model (Figure 3). The RMSE normalized by the mean of observed NO_3 indicated that the deviation between the predicted and observed NO_3 was lowest at Forellenbach, followed by Grosse Ohe and Markungsgraben. The model tended to underestimate NO_3 in the years when the nutrient concentration peaked and the predictors did not explain sufficiently the variation (showing high RMSE) across sites.

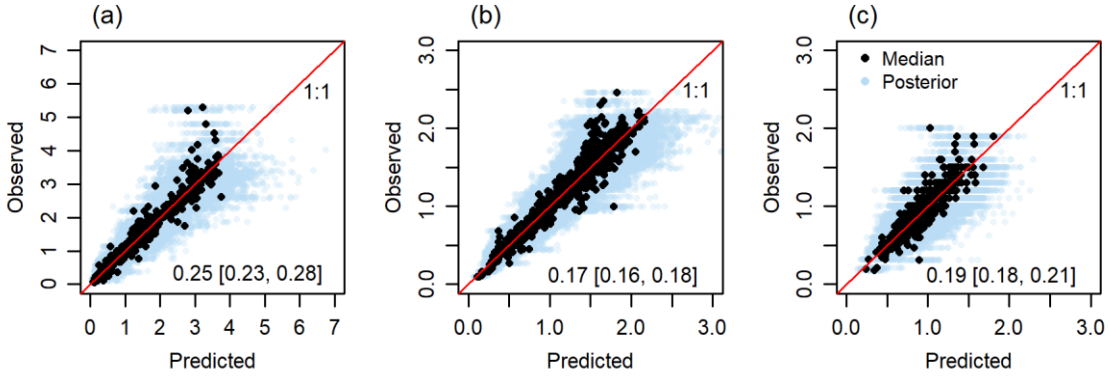

Figure 3. Predicted vs. observed in-stream nitrate (NO_3) concentration of (a) Markungsgraben, (b) Forellenbach and (c) Grosse Ohe. Posterior distributions and medians of predicted NO_3 are displayed. Blue points are random draws from the posterior distribution. 1:1 lines and normalized root mean square errors (median [95 % credible interval]) are indicated.

3.5 Temporal Variations of Model Parameters

The parameter S was estimated for each year by exponentiating the intercept of the regression model based on equation 10 (Figure 4a). S was greatest at Markungsgraben (median of 0.08 – 5.15 mg N L^{-1}), where the NO_3 concentration was generally highest, compared to the medians of 0.05 – 1.97 mg N L^{-1} at Forellenbach and 0.40 – 1.80 mg N L^{-1} at Grosse Ohe. S showed a temporal pattern similar to that of annual mean in-stream NO_3 across the sites with the median ρ of 0.77 – 0.94, increasing in the dieback phase and decreasing in the post-dieback phase. Since S is a complex of multiple parameters (equation 10), we will describe the temporal dynamics further in terms of c_{s0} below (see Equation 11).

The parameter kt_r was significantly ($P(kt_r > 0\ C°^{-1}) < 0.05$) below zero in the pre- and post-dieback phases. kt_r increased close to zero in some years in the middle of the dieback phase (Markungsgraben in 1997 – 1999, Forellenbach in 2003 – 2004 and 2007) (Figure 4b). At Grosse Ohe, the 95 % credible intervals of kt_r remained below zero throughout the study period. The medians of kt_r at Forellenbach and Grosse Ohe remained in the ranges of -0.06 – 0.00 $°C^{-1}$ and -0.04 – -0.02 $°C^{-1}$, respectively. The kt_r at Markungsgraben showed a larger temporal variation compared to those of the other sites. From 2006 onwards, the kt_r at Markungsgraben was -0.10 – -0.05 $°C^{-1}$ (range of medians), considerably lower than at the other sites. The estimate of kt_r was very uncertain in 2012 (-0.07 [-0.13 – -0.02] $°C^{-1}$) because only three data points were available in this year.

The estimates of the C-Q slope b fluctuated near or above zero at Markungsgraben and Grosse Ohe (median -0.08 – 0.21) in their respective pre-dieback and dieback phases (Figure 4c). Medians of the parameter b decreased below zero in the post-dieback phase from 2004 at Markungsgraben and 2012 at Grosse Ohe, although its 95 % credible interval overlapped with zero in some years. At Forellenbach, b was clearly negative in all the years investigated except for 2007 – 2009. These years, in which b was estimated near or above zero (median -0.05 – 0.03), are the last years of the dieback phase at this site.

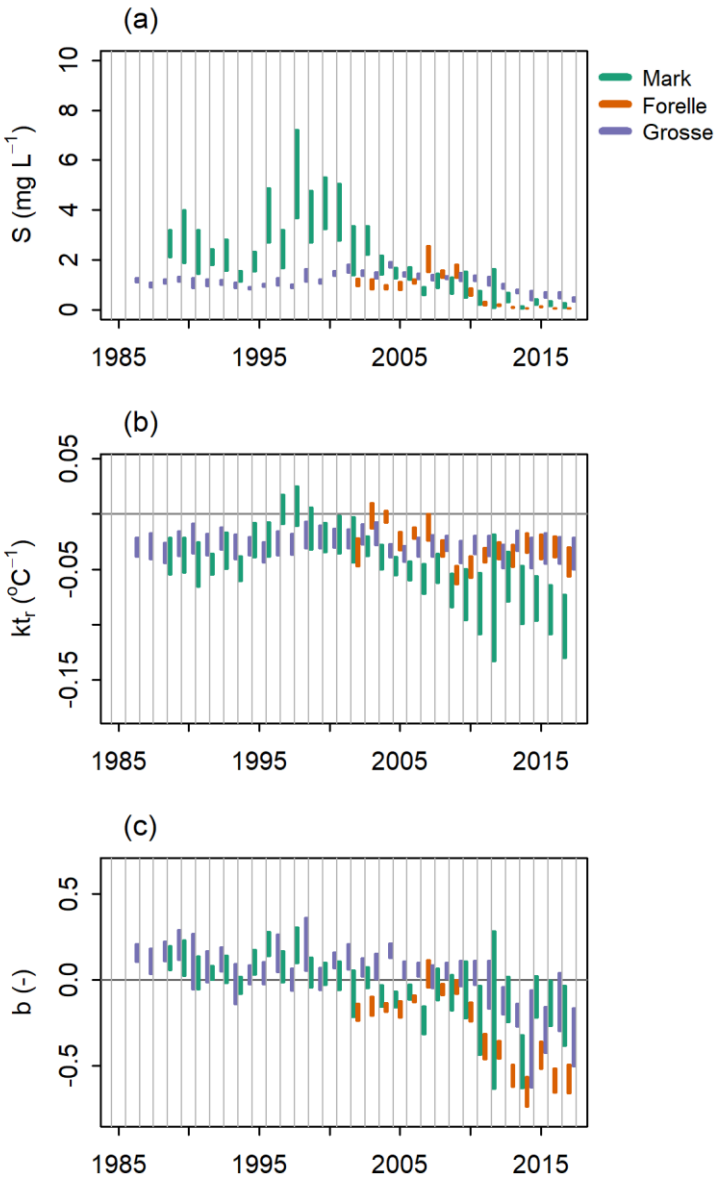

Figure 4. 95 % credible intervals of model parameters (a) S, (b) kt_r and (c) b estimated for each year at Markungsgraben (Mark), Forellenbach (Forelle) and Grosse Ohe (Grosse)

The dynamics of S were broken down into dynamics of c_{s0} using equation 11 given the annual estimations of S and b and for various values of q_0/λ as this ratio was not explicitly estimated (Figure 5). Reasonable values for q_0/λ were chosen based on the range of discharges observed at our study sites. The specific runoff maxima at the study sites were 23.8 – 58.3 mm day^{-1} across the years. Hence, the q_0/λ values were chosen as 20, 40 and 60 mm day^{-1} multiplied by the area of the individual (sub-) catchment. The chosen values of the q_0/λ represent a conservatively wide range of probable maximum discharge. The parameter c_{s0} is positively related with q_0/λ when $b > 0$ and negatively related when $b < 0$ as equation 11 implies. Although c_{s0} varied with different assumptions of q_0/λ (differences in median 0.00 – 1.61 mg N L^{-1}), the general temporal pattern of c_{s0} was not affected by these assumptions.

421 The parameter c_{s0} showed a steep increase at the onset of the dieback in Markungsgraben
422 and less alterations in Forellenbach and Grosse Ohe. At Markungsgraben, c_{s0} rose up to 2.66 –
423 11.62 mg N L^{-1} in 1998 depending on the assumed q_0/λ. At Forellenbach and Grosse Ohe, c_{s0}
424 remained in the ranges of 0.01 – 3.27 mg N L^{-1} and 0.01 – 9.60 mg N L^{-1}, respectively. The c_{s0}
425 estimates of Forellenbach were the lowest among the monitored sites.

426 The estimated c_{s0} peaked in 1998 at Markungsgraben and Grosse Ohe, preceding the peak
427 of in-stream NO_3 (2000 at Markungsgraben and 2003 at Grosse Ohe). Then, c_{s0} decreased below
428 the pre-dieback levels from 2005, 2010 and 2012 onwards at Markungsgraben, Forellenbach and
429 Grosse Ohe, respectively, as the vegetation recovered (Figure 1a). c_{s0} of Markungsgraben
430 showed an especially drastic decrease below pre-dieback levels and even below that of Grosse
431 Ohe.

432 The c_{s0} estimated with $q_0/\lambda = 40$, as an example, was correlated with the annual mean of
433 in-stream NO_3 with a ρ of 0.88 [0.81, 0.92] at Markungsgraben, 0.77 [0.74, 0.80] at Forellenbach
434 and 0.70 [0.61, 0.79] at Grosse Ohe. c_{s0} tented to be higher than in-stream NO_3 until 2004 at
435 Markungsgraben and until 2012 at Grosse Ohe and was similar or lower afterwards at both sites.
436 At Forellenbach, c_{s0} was lower than in-stream NO_3 for most of the research period except in
437 2007 – 2009, when they were comparable to each other.

438

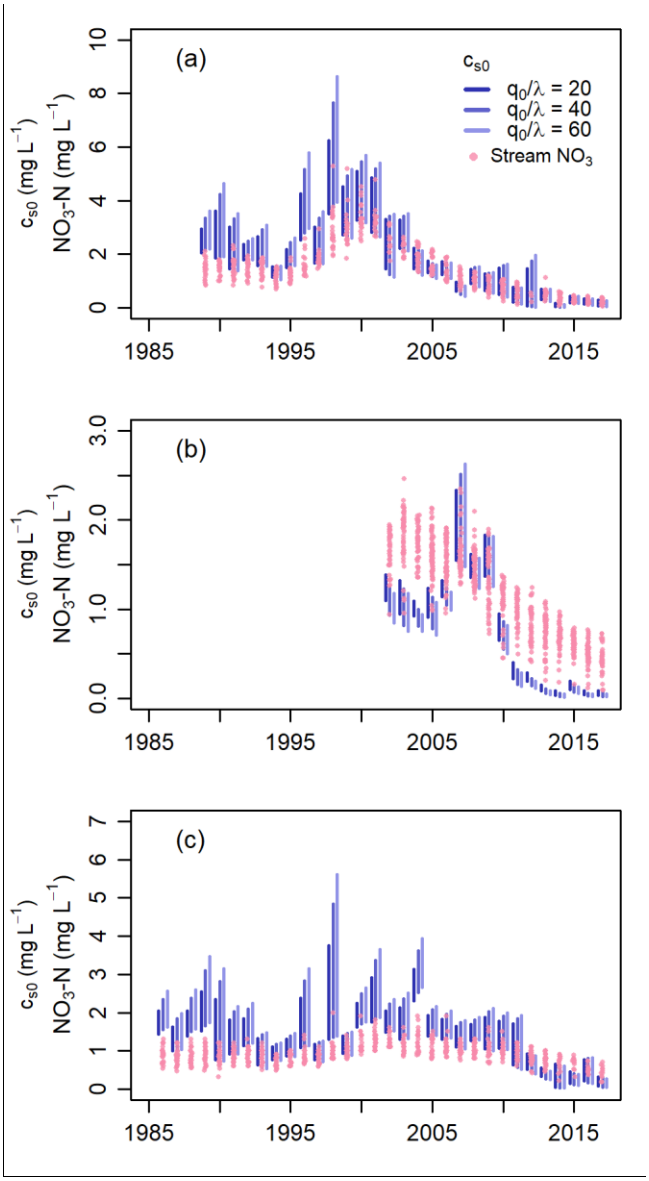

Figure 5. 95 % credible intervals of concentration of nitrate (NO_3) input from hillslope soils to riparian zones (c_{s0}) compared with stream NO_3 concentration at (a) Markungsgraben, (b) Forellenbach and (c) Grosse Ohe. Three c_{s0} scenarios are shown and all convey a similar pattern.

3.6 Correlations between Model Parameters and NDVI

The NDVI was negatively correlated with the annual model parameters, most notably c_{s0}, with correlation coefficients ρ of -0.67 [-0.74, -0.59], -0.81 [-0.85, -0.77] and -0.62 [-0.72, -0.51] at Markungsgraben, Forellenbach and Grosse Ohe, respectively (Figure 6a). The parameter kt_r was negatively related with NDVI at Markungsgraben and Forellenbach with ρ of -0.70 [-0.78 – -0.58] and -0.45 [-0.62 – -0.26], respectively (Figure 6b). At Grosse Ohe, the terrestrial vegetation dynamics did not significantly impact kt_r (ρ of -0.10 [-0.34 – 0.16], with the credible

interval including zero). The correlation between the C-Q slope b and NDVI was -0.31 [-0.45 – -0.11], -0.81 [-0.86 – -0.74] and -0.41 [-0.53 – -0.28] at Markungsgraben, Forellenbach and Grosse Ohe, respectively, with the strongest correlation at Forellenbach (Figure 6c).

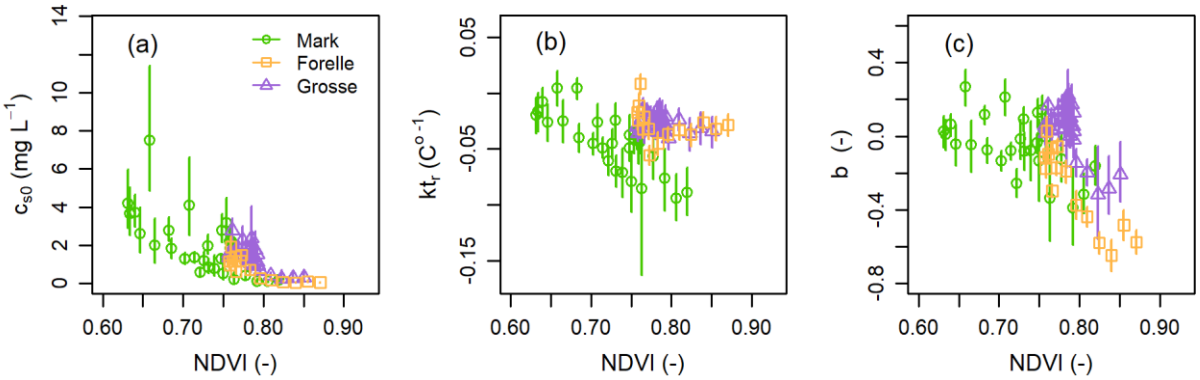

Figure 6. Annual model parameter estimates (a) c_{s0}, (b) b and (c) kt_r for Markungsgraben (Mark), Forellenbach (Forelle) and Grosse Ohe (Grosse) plotted against NDVI. Error bars signify the 95 % credible intervals of the parameters.

4 Discussion

4.1 Dynamics of Catchment Processes Inferred via Time-Varying Model Parameters

4.1.1 Nitrate Inputs to the Riparian Zone

The soil NO_3 (c_{s0}) increased as N was released from the dead trees in the dieback phase and decreased in the post-dieback phase again below pre-dieback levels (Figure 1a,c). c_{s0} showed negative correlation with NDVI (Figure 6a). These results suggest that the soil NO_3 input was affected by the vegetation dynamics. Furthermore, c_{s0} showed high correlations with the annual mean NO_3 concentration (section 3.5), implying that the NO_3 input from the soil governed strongly the in-stream NO_3 concentration.

The reduction of c_{s0} in the post-dieback phase indicates that removal of NO_3 (hydrological export and biological retention) outran supply of NO_3 (decay of the dead trees and atmospheric deposition). Export of NO_3 via stream discharge depleted the nutrient over 7 – 10 years after the diebacks. Additionally, regrowth of young vegetation enhanced net retention of NO_3 as it shed little amounts of litter compared to mature vegetation [*Covington*, 1979; *Bormann and Likens*, 1994]. The strongest dieback in Markungsgraben created large openings and allowed for the establishment and growth of understory vegetation communities [*Niemelä*, 1999], which led to the most active regrowth of the vegetation (Figure 1a) and reduction of c_{s0} (Figure 5).

For comparison, the NO_3 concentration in soil water measured in the Forellenbach catchment by *Beudert and Breit* [2004] rose in 1997 – 2000 up to approximately 45 mg N L^{-1}, 12-fold higher than the maximum c_{s0} estimated at this site (Figure 5). Soil water in that study was collected from a plot with a dead spruce stand upslope of the stream, while c_{s0} in this study

conceptually represents the NO_3 concentration at the soil surface of the whole of the riparian zone. The NO_3 concentration in the riparian zone was reduced compared to the upslope soil water by biogeochemical retention in the unsaturated zone and dilution with groundwater during transit to the riparian zone [*Beudert and Klöcking*, 2007]. Biogeochemical and hydrological processes in the hillslopes also played important roles in the NO_3 export [*Verseveld et al.*, 2009; *Chadwick and Asner*, 2016; *Harms and Ludwig*, 2016], although the catchment model in this study does not explain those processes.

4.1.2 Rates of Biogeochemical Processes in the Riparian Zone

The temporal evolution of NO_3 concentrations and the parameter kt_r in our study catchment reflects how its N budget evolved during the bark beetle outbreak and the subsequent succession. The parameter kt_r was negative in the pre-dieback period, indicating that the riparian zone was a net sink of NO_3. With the dieback, NO_3 was produced at a rate comparable to that of its retention in the riparian zone ($kt_r \approx 0\ C^{\circ -1}$). The riparian zone started to retain NO_3 effectively again in the post-dieback phase, showing negative kt_r.

Vegetation controls N export not only by taking up the nutrient for growth but also by providing a carbon energy source via exudation or litterfall for microbial denitrification [*Scaglia et al.*, 1985; *Mulholland et al.*, 2008; *Dosskey et al.*, 2010; *Zhai et al.*, 2013]. Both processes could have been impaired by the mortality of the trees and recovered with the forest recovery, supported by the correlation between kt_r and NDVI especially in the strongly affected Markungsgraben. While denitrification has been reported as the primary process of NO_3 removal in soil-water systems [*Bachand and Horne*, 1999; *Mulholland et al.*, 2008], *Huber* [2005] attributed the seasonal pattern of NO_3 in our catchment to the active vegetation uptake during summer. However, it was not possible to separate the two pathways of retention with the data available for this study; this will be subject of future research.

With marginal changes in annual precipitation, evapotranspiration was reduced while the runoff coefficient increased in the catchments following the dieback, most remarkable in Markungsgraben [*Beudert and Klöcking*, 2007; *Bernsteinová et al.*, 2015]. The increased runoff coefficient suggests that canopy mortality could have altered the residence time of the nutrient (t_r) and affected the N retention capacity [*Hill et al.*, 1998]. However, this effect could not be separated from the parameter kt_r.

During the dieback phase, organic N and ammonium (NH_4) released from the killed trees were available for mineralization and nitrification, from which more NO_3 was produced in the growing season at high temperatures [*Arheimer et al.*, 1996; *Kaiser et al.*, 2011]. This result supports the first hypothesis that the riparian zone did not act as a net sink of NO_3 and the nutrient export was not retained effectively when the trees were killed. When kt_r was near zero across the sites, the production and retention of NO_3 were of comparable rates so the in-stream NO_3 concentration did not show a seasonal pattern. Such disappearance or even reversal of the seasonal pattern after severe dieback has frequently been observed in forest catchments [*Pardo et al.*, 1995; *Yeakley et al.*, 2003; *Kaňa et al.*, 2015].

In Markungsgraben, NO_3 was depleted thus less available for export in the post-dieback phase (c_{s0} in Figure 5a) and retention was enhanced (Figure 4b) with the recovery of the vegetation (Figure 6c). Thus, we maintain partly the second hypothesis that the nutrient retention

was recovered with the post-dieback regrowth of the forest. In addition, the N input via atmospheric deposition showed a reduction over time in our catchment [*Beudert and Gietl*, 2015], which could have contributed to the decrease in stream NO_3 but was not evaluated in this study.

4.1.3 Hydrological Pathways of Nitrate Export

The C-Q relationship has been interpreted by heterogeneous nutrient sources within a catchment that are variously connected to the stream by dynamic transport pathways [*Seibert et al.*, 2009; *Basu et al.*, 2010]. In a mechanistic sense, the solute is mainly transported via near-surface layers when $b > 0$ or via sub-surface layers when $b < 0$ [*Seibert et al.*, 2009]. The in-stream solute concentration increases at high flows ($b > 0$) as ground water intersects near-surface layers rich in the nutrient (flushing pattern) (see equations 10 and 11). Conversely, when $b < 0$, then the solute concentration decreases at high flows as the water flux in near-surface layers does not flush a high concentration of solute (dilution pattern). A value for b near zero indicates that the solute transport is homogeneous over the depth of the riparian zone and does not vary with discharge (chemostasis). However, *Musolff et al.* [2015] found empirically that chemostatic solute export has b values in the range of [-0.2, 0.2]. The C-Q relationship can vary if the dominant pathway of nutrient export is switched [*Zhi et al.*, 2019]. In our catchment, the temporal variations of b and c_{s0} suggest that the NO_3 export was chemostatic in the pre-dieback and dieback phases and shifted to a dilution pattern in the post-dieback period.

The parameter b was in the range of [-0.2, 0.2] at Markungsgraben and Grosse Ohe in the pre-dieback phase (Figure 4c) indicating chemostasis of the NO_3 export. Several studies observed that chemostasis of NO_3 is a sign of N-saturation with the nutrient homogeneously distributed [*Basu et al.*, 2010; *Van Meter and Basu*, 2015; *Bieroza et al.*, 2018]. The parameter b was near zero when the parameter c_{s0} was estimated comparable to in-stream NO_3, supporting indirectly the homogeneous distribution of NO_3 in the soil profile of the riparian zone (Figure 5). Conversely, b was slightly above zero when c_{s0} was higher than in-stream NO_3. The parameters b and c_{s0} were especially high in the dieback phase (Figure 4a,c) showing high correlations with NDVI (Figure 6c). In these years, NO_3 released from the killed trees accumulated in the near-surface layer inducing a flushing effect and hence steep increases in c_{s0}.

The parameter b decreased below zero (Figure 4) and c_{s0} was lower than the stream NO_3 (Figure 5) in the post-dieback phase (after 2014 at Markungsgraben and after 2013 at Grosse Ohe). By that time, the NO_3 concentration in the near-surface layer had been depleted by the flushing and the biological retention. It is also likely that the NO_3 had been leaching into deeper groundwater over time after the diebacks [*Jury and Nielsen*, 1989]. The water flux through the near-surface layer at high flows then diluted the stream NO_3, resulting in the negative C-Q slopes observed.

The parameter b was lowest at Forellenbach and clearly negative in the pre- and post-dieback periods, signifying a strong dilution effect in this sub-catchment. Indeed, the NO_3 concentration decreased sharply in storm events. This dilution effect is supported by the high baseflow index of 64 % possibly caused by flat topography (section 3.1). In 2007 – 2009, during the second dieback (Figure 1a), b was near zero and c_{s0} was comparable to in-stream NO_3, likely because the released nutrient was distributed homogeneously along the soil profile. In the post-

dieback phase, NO_3 was depleted in the near-surface layer, thus b was decreased below zero and pre-dieback levels and c_{s0} was much lower than in-stream NO_3.

4.2 Concentration-Discharge-Temperature Relationship

Regression modeling predicting NO_3 concentrations in streams from air or water temperature as a single predictor has been used elsewhere [e.g. *Clark et al.*, 2004a; *Exner-Kittridge et al.*, 2016]. A negative C-T relationship is attributed to reduced microbial and plant uptake of the nutrient at low temperatures [*Clark et al.*, 2004a]. However, more common by far is the C-Q model, which is often interpreted by the variability of solute exports coming from spatially heterogeneous sources and mobilized through temporally varying pathways [e.g. *Seibert et al.*, 2009; *Basu et al.*, 2010; *Musolff et al.*, 2015; *Moatar et al.*, 2017; *Zhi et al.*, 2019]. *Winterdahl et al.* [2011] revealed that soil temperature was an important factor responsible for the residuals of a C-Q model for DOC (dissolved organic carbon). They modified the C-Q model by *Seibert et al.* [2009] to allow the profile of concentration to vary as a function of soil temperature. The current study found that the C-Q-T model predicted NO_3 export more accurately than either the C-T or the C-Q model (Table S1). The rationale of the model developed in this study (section 3.3) explains the mechanism of the empirical C-Q-T relationship, complementing the attempt by *Winterdahl et al.* [2011].

Basu et al. [2011] and *Thompson et al.* [2011] classified solute export from a catchment into source-limited and transport-limited states. Previous studies suggested different metrics for verifying the state of solute export such as the parameter b, coefficients of variance (CV) and r^2 of the load-discharge regression [*Godsey et al.*, 2009; *Basu et al.*, 2010; *Musolff et al.*, 2015]. In our study, shifts between these states were verified based on the annual estimates of the parameters kt_r, b and c_{s0} of the C-Q-T model. The NO_3 export was in a transport-limited state in the pre-dieback phase, revealed by its chemostasis ($-0.2 \leq b \leq 0.2$). However, the riparian zone acted as a net sink of NO_3 ($kt_r < 0$ $C^{\circ -1}$; c_{s0} higher than in-stream NO_3), and in-stream NO_3 was stagnant, indicating an equilibrium between export and retention of NO_3. In the dieback phase, the nutrient export was exacerbated with the release of the N from the killed trees (increased c_{s0}) without net retention ($kt_r \approx 0$ $C^{\circ -1}$). As the N was depleted and the forest recovered in the post-dieback phase, the nutrient export was shifted to a source-limited state with strong N retention (low negative $kt_r < 0$ $C^{\circ -1}$), and the lowered NO_3 transport in the near-surface layer ($b < 0$; lowered c_{s0}).

4.3 Efficacy of Bayesian Hierarchical Modelling

Previous studies of the C-Q model revealed that its parameters vary temporally [*Köhler et al.*, 2008; *Seibert et al.*, 2009]. The C-Q-T model of our study was fit to the data in a Bayesian hierarchical framework to allow for the temporal variability of its parameters, which explained the temporal changes in the catchment processes caused by the forest dieback. The partially pooled model captured the variations in the relationships between the variables and showed an enhancement in accuracy compared to the pooled regression models (Table 1) [*Simpson*, 1951; *Cha et al.*, 2016]. A next level of model development would be the prediction of parameter variations, as *Cha et al.* [2017] demonstrated, with data of vegetation dynamics, for instance NDVI in our case.

A Bayesian hierarchical model is capable of predicting the response variable and parameters by sharing information across hierarchical levels and at the same time avoiding overfitting [*Borsuk et al.,* 2001]. At Markungsgraben, NO_3 and the parameters for 2012 were predicted with three data points only, albeit yielding low precision in the parameter estimates. Had the model been applied in a non-pooling approach, the estimations would have been over-confident given the little amount of the data.

5 Conclusions

In our case study, the best fitting regression model predicted stream NO_3 concentration (C) with discharge (Q) and water temperature (T). This C-Q-T relationship adds to the widely acknowledged C-Q relationship the effect of water temperature on the variability of solutes in streams. The C-Q-T relationship could be applicable to other non-conservative solutes that are regulated by biogeochemical reactions in streams, and hence are sensitive to water temperature. It would be worthwhile to investigate the applicability of the C-Q-T model to different solutes and types of catchments.

The top-down modeling approach yielded mechanistic interpretations of soil N inputs, main transport pathways and rates of biogeochemical processes in a parsimonious way that is commensurate with the data availability. Due to its flexibility, Bayesian hierarchical modeling is especially suited for top-down modelling via time-varying parameters. Partial pooling maintains flexibility of model parameters while avoiding over-fitting. The next step following the top-down route would be to explicitly model the annual variation of parameters by auxiliary data, such as NDVI as indicated in our study.

The temporal trends of the parameters led us to maintain our first hypothesis that the NO_3 released through tree mortality (increased c_{s0}) was not effectively retained in the riparian zone during the dieback phase ($kt_r \geq 0\ C^{o-1}$). In the post-dieback phase, NO_3 was depleted (decreased c_{s0}) and young re-growing vegetation retained more NO_3 than it released N via litter shedding ($kt_r < 0\ C^{o-1}$), thus we partly maintain our second hypothesis. We attribute the changes in the NO_3 budget to the alteration in the nutrient retention capacity of the riparian zone but also to abrupt release and depletion of the nutrient. The hypotheses could be tested robustly by means of the parameters estimated as probability distributions in the Bayesian hierarchical framework.

Although the bark beetle induced forest dieback observed in our study catchment impaired the water quality by releasing N from the forest, the system turned out resilient in the sense of a rapid recovery of ecosystem functions (i.e., retaining nutrients). It is important to note here that the system was not managed at all. Stream NO_3 concentrations were reduced 10 years after the dieback in the most severely affected upper sub-catchments and showed a general high resistance in the most downstream reach (Figure 2). Moreover, the biodiversity in our forest catchment was improved after the diebacks with the emergence of new habitats provided by standing and lying deadwood [*Beudert et al.,* 2014]. Hence, our study supports that European montane spruce forests are in fact highly resilient to the current disturbance regime [*Zeppenfeld et al.,* 2015; *Senf et al.,* 2019]; we here complement these studies by showing that this resilience also includes the key ecosystem function of water purification.

The water temperature in our catchment showed a constantly increasing trend presumably as a manifestation of climate change [*Beudert et al.,* 2018]. An increase in forest mortality is

expected under climate change [*Allen et al.*, 2010; *Seidl et al.*, 2017], with more frequent forest diebacks that might also increase in severity. Hence, under climate change more nutrients might be released. A portion of the released N would be denitrified and released into the atmosphere as nitrous oxide (N_2O) [*Norton et al.*, 2015], a potent greenhouse gas. It would be shortsighted to limit N cycling studies to water quality effects ignoring the climate change potential of N_2O emissions. Further studies are needed to explore the response of the N cycle of forest catchments to changing mortality patterns under climate change.

Acknowledgments and Data Availability

BB designed and performed the hydrochemical monitoring program of Forellenbach and coordinated the related programs of Grosse Ohe catchment in the Bavarian Forest National Park. CS contrived the methods for the statistical analyses of the data. HJ formulated research questions, developed the codes for the statistical analyses and performed the analysis. HJ and TK developed the mechanistic catchment model. HJ led the writing of the paper which all co-authors contributed to. The work of HJ was part of his doctoral research at IRI THESys of Humboldt-Universität zu Berlin, enrolled at the Geography Departed of the same university. IRI THESys was funded by the German Excellence Initiative. The hydrochemical data were provided from the Bavarian Environment Agency (LFU) and the German Federal Environment Agency (UBA) and are available online in Zenodo repository (https://doi.org/10.5281/zenodo.3703070) [*Beudert et al.*, 2020].

References

Adams, H. D., C. H. Luce, D. D. Breshears, C. D. Allen, M. Weiler, V. C. Hale, A. M. S. Smith, and T. E. Huxman (2012), Ecohydrological consequences of drought-and infestation-triggered tree die-off: insights and hypotheses, *Ecohydrology*, *5*(2), 145-159.

Allen, C. D., et al. (2010), A global overview of drought and heat-induced tree mortality reveals emerging climate change risks for forests, *Forest ecology and management*, *259*(4), 660-684. https://doi.org/10.1016/j.foreco.2009.09.001

Arheimer, B., L. Andersson, and A. Lepistö (1996), Variation of nitrogen concentration in forest streams—influences of flow, seasonality and catchment characteristics, *Journal of Hydrology*, *179*(1-4), 281-304. 10.1016/0022-1694(95)02831-5

Bachand, P. A. M., and A. J. Horne (1999), Denitrification in constructed free-water surface wetlands: II. Effects of vegetation and temperature, *Ecological Engineering*, *14*(1-2), 17-32. 10.1016/S0925-8574(99)00017-8

Basu, N. B., S. E. Thompson, P. Suresh, and C. Rao (2011), Hydrologic and biogeochemical functioning of intensively managed catchments: A synthesis of top-down analyses, *Water Resources Research*, *47*.

Basu, N. B., et al. (2010), Nutrient loads exported from managed catchments reveal emergent biogeochemical stationarity, *Geophysical Research Letters*, *37*, L23404.

Bernsteinová, J., C. Bässler, L. Zimmermann, J. Langhammer, and B. Beudert (2015), Changes in runoff in two neighbouring catchments in the Bohemian Forest related to climate and land

cover changes, *Journal of Hydrology and Hydromechanics*, *63*(4), 342-352. 10.1515/johh-2015-0037

Betts, E. F., and J. B. Jones Jr. (2009), Impact of wildfire on stream nutrient chemistry and ecosystem metabolism in boreal forest catchments of interior Alaska, *Arctic, Antarctic, and Alpine Research*, *41*(4), 407-417.

Beudert, B., and W. Breit (2004), Zwölf Jahre Integrated-Monitoring-Programm an der Meßstelle Forellenbach im Nationalpark Bayerischer Wald, *Fkz*, *351*(1), 12.

Beudert, B., and B. Klöcking (2007), Grosse Ohe: impact of bark beetle infestation on the water and matter budget of a forested catchment, in *Forest hydrology: results of research in Germany and Russia*, edited by R. Schwarze and S. V. Marunich, IHP/HWRP-Sekretariat, Koblenz.

Beudert, B., and G. Gietl (2015), Long-term monitoring in the Große Ohe catchment, Bavarian Forest National Park, *Silva Gabreta*, *21*(1), 5-27.

Beudert, B., J. Bernsteinová, J. Premier, and C. Bässle (2018), Natural disturbance by bark beetle offsets climate change effects on streamflow in headwater catchments of the Bohemian Forest, *Silva Gabreta*, *24*, 21-45.

Beudert, B., H. Jung, C. Senf, and T. Krueger (2020), Water quality and discharge monitoring data in Bavarian Forest National Park, Germany, edited, Zenodo. https://doi.org/10.5281/zenodo.3703070

Beudert, B., C. Bässler, S. Thorn, R. Noss, B. Schröder, H. Dieffenbach-Fries, N. Foullois, and J. Müller (2014), Bark beetles increase biodiversity while maintaining drinking water quality, *Conservation Letters*, *8*(4), 272-281.

Biederman, J. A., T.Meixner, A. A. Harpold, D. E. Reed, E. D. Gutmann, J. A. Gaun, and P. D. Brooks (2016), Riparian zones attenuate nitrogen loss following bark beetle-induced lodgepole pinemortality, *J. Geophys. Res. Biogeosci.*, *121*. 10.1002/2015JG003284

Bieroza, M. Z., A. L. Heathwaite, M. Bechmann, K. Kyllmar, and P. Jordan (2018), The concentration-discharge slope as a tool for water quality management, *Science of the Total Environment*, *630*, 738-749.

Bormann, F. H., and G. Likens (1994), *Pattern and process in a forested ecosystem*, Springer, New York. http://10.1007/978-1-4612-6232-9

Borsuk, M. E., D. Higdon, C. A. Stow, and K. H. Reckhow (2001), A Bayesian hierarchical model to predict benthic oxygen demand from organic matter loading in estuaries and coastal zones, *Ecological modelling*, *143*, 165-181. https://doi.org/10.1016/S0304-3800(01)00328-3

Botter, G., N. B. Basu, S. Zanardo, P. S. C. Rao, and A. Rinaldo (2010), Stochastic modeling of nutrient losses in streams: Interactions of climatic, hydrologic, and biogeochemical controls, *Water Resources Research*, *46*, W08509.

Carpenter, B., A. Gelman, M. D. Hoffman, D. Lee, B. Goodrich, M. Betancourt, M. Brubaker, J. Guo, P. Li, and A. Riddell (2017), Stan: A probabilistic programming language, *Journal of Statistical Software*, *76*(1). https://doi.org/10.18637/jss.v076.i01

Cha, Y., S. S. Park, H. W. Lee, and C. A. Stow (2016), A Bayesian hierarchical approach to model seasonal algal variability along an upstream to downstream river gradient, *Water Resources Research*, *52*, 348-357. 10.1002/2015WR017327

Cha, Y., K. H. Cho, H. Lee, T. Kang, and J. H. Kim (2017), The relative importance of water temperature and residence time in predicting cyanobacteria abundance in regulated rivers, *Water Research*, *124*, 11-19. http://http://dx.doi.org/10.1016/j.watres.2017.07.040

742 Chadwick, K. D., and G. P. Asner (2016), Tropical soil nutrient distributions determined by
743 biotic and hillslope processes, *Biogeochemistry*, *127*(2-3), 273-289.
744 https://doi.org/10.1007/s10533-015-0179-z
745 Chavez, F. P., and S. K. Service (1996), Temperature-nitrate relationships in the central and
746 eastern tropical Pacific, *Journal of Geophysical Research*, *101*(C9), 20553-20563.
747 Christensen, P. B., L. P. Nielsen, J. Sørensen, and N. P. Revsbech (1990), Denitrification in
748 nitrate-rich streams: Diurnal and seasonal variation related to benthic oxygen metabolism,
749 *Limnology and Oceanography*, *35*(3), 640-651. 10.4319/lo.1990.35.3.0640
750 Clark, M. J., M. S. Cresser, R. Smart, P. J. Chapman, and A. C. Edwards (2004a), The influence
751 of catchment characteristics on the seasonality of carbon and nitrogen species concentrations in
752 upland rivers of Northern Scotland, *Biogeochemistry*, *68*(1), 1-19.
753 10.1023/B:BIOG.0000025733.07568.11
754 Clark, M. J., M. S. Cresser, R. Smart, P. J. Chapman, and A. C. Edwards (2004b), The influence
755 of catchment characteristics on the seasonalitz of carbon and nitrogen species concentrations in
756 upland rivers of Northern Scotland, *Biogeochemistry*, *68*, 1-19.
757 Covington, W. W. (1979), Forest floor organic matter and nutrient content and leaf fall during
758 secondary succession in northern hardwoods, 99 pp, Yales University, New Haven, CT.
759 Dosskey, M. G., P. Vidon, N. P. Gurwick, C. J. Allan, T. P. Duval, and R. Lowrance (2010), The
760 role of riparian vegetation in protecting and improving chemical water quality in streams,
761 *Journal of the American Water Resources Association*, *46*(2), 261-277.
762 Exner-Kittridge, M., P. Strauss, C. n. Bl;schl, A. Eder, E. Saracevic, and M. Zessner (2016), The
763 seasonal dynamics of the stream sources and input flow paths of water and nitrogen of an
764 Austrian headwater agricultural catchment, *Science of the Total Environment*, *542*, 935-945.
765 http://dx.doi.org/10.1016/j.scitotenv.2015.10.151
766 EcoHydRology: A Community Modeling Foundation for Eco-Hydrology
767 Gall, H. E., J. Park, C. J. Harman, J. W. Jawitz, and P. S. C. Rao (2013), Landscape filtering of
768 hydrologic and biogeochemical responses in managed catchments, *Landscape Ecology*, *28*, 651-
769 664.
770 Gelman, A. (2006), Prior distributions for variance parameters in hierarchical models (comment
771 on article by Browne and Draper), *Bayesian analysis*, *1*(3), 515-534.
772 Godsey, S. E., J. W. Kirchner, and D. W. Clow (2009), Concentration–discharge relationships
773 reflect chemostatic characteristics of US catchments, *Hydrological Processes: An International*
774 *Journal*, *23*(13), 1844-1864.
775 Gundersen, P., I. K. Schmidt, and K. Raulund-Rasmussen (2006), Leaching of nitrate from
776 temperate forests effects of air pollution and forest management, *Environmental reviews*, *14*(1),
777 1-57. https://doi.org/10.1139/a05-015
778 Hansen, M. C., et al. (2013), High-resolution global maps of 21st-century forest cover change,
779 *Science*, *342*(850-853). http://10.1126/science.1244693
780 Harman, C. J., P. S. C. Rao, N. B. Basu, G. S. McGrath, P. Kumar, and M. Sivapalan (2011),
781 Climate, soil, and vegetation controls on the temporal variability of vadose zone transport, *Water*
782 *Resources Research*, *47*, W00J13.
783 Harms, T. K., and S. M. Ludwig (2016), Retention and removal of nitrogen and phosphorus in
784 saturated soils of arctic hillslopes, *Biogeochemistry*, *127*(2-3), 291-304.
785 https://doi.org/10.1007/s10533-016-0181-0

786 Hartmann, A., J. Kobler, M. Kralik, T. Dirnböck, F. Humer, and M. Weiler (2016), Model-aided
787 quantification of dissolved carbon and nitrogen release after windthrow disturbance in an
788 Austrian karst system, *Biogeosciences*, *131*(159-174). https://doi.org/10.5194/bg-13-159-2016
789 Heurich, M., T. Ochs, T. Andresen, and T. Schneider (2010), Object-orientated image analysis
790 for the semi-automatic detection of dead trees following a spruce bark beetle (Ips typographus)
791 outbreak, *European Journal of Forest Research*, *129*(3), 313-324.
792 https://doi.org/10.1007/s10342-009-0331-1
793 Hill, A. R., C. F. Labadia, and K. Sanmugadas (1998), Hyporheic zone hydrology and nitrogen
794 dynamics in relation to the streambed topography of a N-rich stream, *Biogeochemistry*, *42*(3),
795 285-310.
796 Hilton, J., M. O'Hare, M. J. Bowes, and J. I. Jones (2006), How green is my river? A new
797 paradigm of eutrophication in rivers, *Sci. Total. Environ.*, *365*(1-3), 66–83.
798 https://doi.org/10.1016/j.scitotenv.2006.02.055
799 Huber, C. (2005), Long lasting nitrate leaching after bark beetle attack in the highlands of the
800 Bavarian Forest National Park, *Journal of environmental quality*, *34*(5), 1772-1779.
801 Jury, W. A., and D. R. Nielsen (1989), Nitrate transport and leaching mechanisms, in
802 *Developments in Agricultural and Managed Forest Ecology*, edited by R. F. Follett, pp. 1-395,
803 Elsevier.
804 Kaiser, C., et al. (2011), Plants control the seasonal dynamics of microbial N cycling in a beech
805 forest soil by belowground C allocation, *Ecology*, *92*(5), 1036-1051.
806 Kaňa, J., K. Tahovská, J. Kopáček, and H. Šantrůčková (2015), Excess of Organic Carbon in
807 Mountain Spruce Forest Soils after Bark Beetle Outbreak Altered Microbial N Transformations
808 and Mitigated N-Saturation, *PloS one*, *10*(7). https://doi.org/10.1371/journal.pone.0134165
809 Kautz, M., K. Dworschak, A. Gruppe, and R. Schopf (2011), Quantifying spatio-temporal
810 dispersion of bark beetle infestations in epidemic and non-epidemic conditions, *Forest Ecology*
811 *and Management*, *262*(4), 598-608. https://doi.org/10.1016/j.foreco.2011.04.023
812 Köhler, S. J., I. Buffam, H. Laudon, and K. H. Bishop (2008), Climate's control of intra-annual
813 and interannual variability of total organic carbon concentration and flux in two contrasting
814 boreal landscape elements, *Journal of Geophysical Research: Biogeosciences*, *113*(G3).
815 https://doi.org/10.1029/2007JG000629
816 Krueger, T., J. Freer, J. N. Quinton, and C. J. A. Macleod (2007), Processes affecting transfer of
817 sediment and colloids, with associated phosphorus, from intensively farmed grasslands: a critical
818 note on modelling of phosphorus transfers, *Hydrological processes*, *21*, 557-562.
819 https://doi.org/10.1002/hyp.6596
820 Lowrence, R. R., R. L. Todd, and L. E. Asmussen (1983), Waterborne nutrient budgets for the
821 riparian zone of an agricultural watershed, *Agriculture, ecosystems & environment*, *10*(4), 371-
822 384. https://doi.org/10.1016/0167-8809(83)90088-9
823 Masclaux-Daubresse, C., F. Daniel-Vedele, J. Dechorgnat, F. Chardon, L. Gaufichon, and A.
824 Suzuki (2010), Nitrogen uptake, assimilation and remobilization in plants: challenges for
825 sustainable and productive agriculture, *Annals of botany*, *105*(7), 1141-1157.
826 https://doi.org/10.1093/aob/mcq028
827 Moatar, F., B. W. Abbott, C. Minaudo, F. Curie, and G. Pinay (2017), Elemental properties,
828 hydrology, and biology interact to shape concentration-discharge curves for carbon, nutrients,
829 sediment, and major ions, *Water Resources Research*, *53*, 1270-1287. 10.1002/2016WR019635
830 Mulholland, P. J., et al. (2008), Stream denitrification across biomes and its response
831 to anthropogenic nitrate loading, *Nature Letters*, *452*(7184), 202. doi:10.1038/nature06686

Musolff, A., C. Schmidt, B. Selle, and J. H. Fleckenstein (2015), Catchment controls on solute export, *Advances in Water Resources*, *86*, 133-146.

Niemelä, J. (1999), Management in relation to disturbance in the boreal forest, *Forest Ecology and Management*, *115*(2-3), 127-134. https://doi.org/10.1016/S0378-1127(98)00393-4

Norton, U., B. E. Ewers, B. Borkhuu, N. R. Brown, and E. Pendall (2015), Soil nitrogen five years after bark beetle infestation in lodgepole pine forests, *Soil Science Society of America Journal*, *79*(1), 282-293. http://10.2136/sssaj2014.05.0233

Obenour, D. R., A. D. Gronewold, C. A. Stow, and D. Scavia (2014), Using a Bayesian hierarchical model to improve Lake Erie cyanobacteria bloom forecasts, *Water Resources Research*, *50*, 7847-7860. 10.1002/2014WR015616.

Pardo, L. H., C. T. Driscoll, and G. E. Likens (1995), Patterns of nitrate loss from a chronosequence of clear-cut watersheds, *Water, air, and soil pollution*, *85*(3), 1659-1664. https://doi.org/10.1007/BF00477218

Parkyn, S. (2004), *Review of riparian buffer zone effectiveness*, Ministry of Agriculture and Forestry, Wellington, New Zealand.

R Core Team (2018). R: A language and environment for statistical computing. R Foundation for Statistical Computing, Vienna, Austria. URL https://www.R-project.org/.

Rose, L. A., D. L. Karwan, and S. E. Godsey (2018), Concentration–discharge relationships describe solute and sediment mobilization, reaction, and transport at event and longer timescales, *Hydrological processes*, *32*(18), 2829-2844. https://doi.org/10.1002/hyp.13235

Scaglia, J., R. Lensi, and A. Chalamet (1985), Relationship between photosynthesis and denitrification in planted soil, *Plant and Soil*, *84*(1), 37-43.

Seibert, J., T. Grabs, S. Köhler, H. Laudon, M. Winterdahl, and K. Bishop (2009), Linking soil- and stream-water chemistry based on a Riparian Flow-Concentration Integration Model, *Hydrology and Earth System Sciences*, *13*, 2287-2297.

Seidl, R., M. J. Schelhaas, and M. J. Lexer (2011), Unraveling the drivers of intensifying forest disturbance regimes in Europe, *Global Change Biology*, *17*(9), 2842-2852. https://doi.org/10.1111/j.1365-2486.2011.02452.x

Seidl, R., et al. (2017), Forest disturbances under climate change, *Nature Climate Change*, *7*(6), 395. http://10.1038/nclimate3303

Senf, C., J. Müller, and R. Seidl (2019), Post-disturbance recovery of forest cover and tree height differ with management in Central Europe, *Landscape Ecology*, *34*(12), 2837-2850. https://doi.org/10.1007/s10980-019-00921-9

Senf, C., D. Pflugmacher, P. Hostert, and R. Seidl (2017), Using Landsat time series for characterizing forest disturbance dynamics in the coupled human and natural systems of Central Europe, *ISPRS Journal of Photogrammetry and Remote Sensing*, *130*, 453-463. https://doi.org/10.1016/j.isprsjprs.2017.07.004

Senf, C., D. Pflugmacher, Y. Zhiqiang, J. Sebald, J. Knorn, M. Neumann, P. Hostert, and R. Seidl (2018), Canopy mortality has doubled in Europe's temperate forests over the last three decades, *Nature communications*, *9*(1), 4978.

Simpson, E. H., , J. R. Stat. Soc., Ser. B, 13(2), 238–241. (1951), The interpretation of interaction in contingency tables, *Journal of the Royal Statistical Society: Series B (Methodological)*, *13*(2), 238-241. 10.1111/j.2517-6161.1951.tb00088.x

Sivapalan, M., G. Blöschl, L. Zhang, and R. Vertessy (2003), Downward approach to hydrological prediction, *Hydrological processes*, *17*(11), 2010-2111.

877 Stan Development Team (2018), Stan Development Team. 2018. RStan: the R interface to Stan.
878 R package version 2.17.3. http://mc-stan.org.
879 Stoddard, J. L. (1994), Long-term changes in watershed retention of nitrogen: its causes and
880 aquatic consequences, in *Environmental Chemistry of Lakes and Reservoirs*, edited by L. A.
881 Baker, pp. 223-284, ACS Advances in Chemistry Series. http://10.1021/ba-1994-0237.ch008
882 Stow, C. A., and D. Scavia (2008), Modeling hypoxia in the Chesapeake Bay: ensemble
883 estimation using a Bayesian hierarchical model, *Journal of Marine Systems*, *76*(1-2), 244-250.
884 https://doi.org/10.1016/j.jmarsys.2008.05.008
885 Svoboda, M., S. Fraver, P. Janda, R. Bače, and J. Zenáhlíková (2010), Natural development and
886 regeneration of a Central European montane spruce forest, *Forest Ecology and Management*,
887 *260*(5), 707-714. https://doi.org/10.1016/j.foreco.2010.05.027
888 Thompson, S. E., N. B. Basu, J. L. Jr., A. Aubeneau, and P. S. C. Rao (2011), Relative
889 dominance of hydrologic versus biogeochemical factors on solute export across impact gradients,
890 *Water Resources Research*, *47*, W00J05.
891 Van Meter, K. J., and N. B. Basu (2015), "Catchment legacies and time lags: A parsimonious
892 watershed model to predict the effects of legacy storage on nitrogen export, *PLoS One*, *10*(5),
893 e0125971. 10.1371/journal.pone.0125971
894 Vehtari, A., A. Gelman, and J. Gabry (2017), Practical Bayesian model evaluation using leave-
895 one-out cross-validation and WAIC, *Statistics and computing*, *27*(5), 1413-1432.
896 http://dx.doi.org/10.1007/s11222-016-9709-3
897 Verseveld, W. J. v., J. J. McDonnell, and K. Lajtha (2009), The role of hillsope hydrology in
898 controlling nutrient loss, *Journal of Hydrology*, *367*, 177-187.
899 https://doi.org/10.1016/j.jhydrol.2008.11.002
900 Vitousek, P. M., and W. A. Reiners (1975), Ecosystem succession and nutrient retention: a
901 hypothesis, *BioScience*, *25*(6), 376-381.
902 Webb, J. A., M. J. S. Ardson, and W. M. Koster (2010), Detecting ecological responses to flow
903 variation using Bayesian hierarchical models, *Freshwater Biology*, *55*, 108-126. 10.1111/j.1365-
904 2427.2009.02205.x
905 Wetzel, R. (2001), *Limnology: Lake and river ecosystems*, 3rd ed., Academic Press, San Diego,
906 CA.
907 Winterdahl, M., M. Futter, S. Köhler, H. Laudon, J. Seibert, and K. Bishop (2011), Riparian soil
908 temperature modification of the relationship between flow and dissolved organic carbon
909 concentration in a boreal stream, *Water Resources Research*, *47*(8), W08532.
910 https://doi.org/10.1029/2010WR010235
911 Xia, Y., D. E. Weller, M. N. Williams, T. E. Jordan, and X. Yan (2016), Using Bayesian
912 hierarchical models to better understand nitrate sources and sinks in agricultural watersheds,
913 *Water Research*, *105*, 527-539. http://dx.doi.org/10.1016/j.watres.2016.09.033
914 Xu, H., H. W. Paerl, B. Qin, G. Zhu, N. S. Hall, and Y. Wu (2014), Determining critical nutrient
915 thresholds needed to control harmful cyanobacterial blooms in eutrophic Lake Taihu, China,
916 *Environ. Sci. Technol.*, *49*(2), 1051–1059. https://doi.org/10.1021/es503744q
917 Yeakley, J. A., D. C. Coleman, B. L. Haines, B. D. Kloeppel, J. L. Meyer, W. T. Swank, B. W.
918 Argo, J. M. Deal, and S. F. Taylor (2003), Hillslope nutrient dynamics following upland riparian
919 vegetation disturbance, *Ecosystems*, *6*(2), 154-167. 10.1007/s10021-002-0116-6
920 Zeppenfeld, T., M. Svoboda, R. J. DeRose, M. Heurich, J. Müller, P. Čížková, M. Starý, R.
921 Bače, and D. C. Donato (2015), Response of mountain Picea abies forests to stand-replacing bark

beetle outbreaks: neighbourhood effects lead to self-replacement, *Journal of Applied Ecology*, *52*(5), 1402-1411. https://doi.org/10.1111/1365-2664.12504

Zhai, X., N. Piwpuan, C. A. Arias, T. Headley, and H. Brix (2013), Can root exudates from emergent wetland plants fuel denitrification in subsurface flow constructed wetland systems?, *Ecological Engineering*, *61*(Part B), 555-563. 10.1016/j.ecoleng.2013.02.014

Zheng, L., M. Bayani, Cardenas, and L. Wang (2016), Temperature effects on nitrogen cycling and nitrate removal-production efficiency in bed form-induced hyporheic zones, *Journal of Geophysical Research: Beogeosciences*, *121*, 1086-1103. http://dx.doi.org/10.1002/2015JG003162

Zhi, W., L. Li, W. Dong, W. Brown, J. Kaye, C. Steefel, and K. H. Williams (2019), Distinct source water chemistry shapes contrasting concentration-discharge patterns, *Water Resources Research*. 10.1029/2018WR024257